

Modeling human health characterization factors for indoor nanomaterial emissions in life cycle assessment: A case-study of titanium dioxide

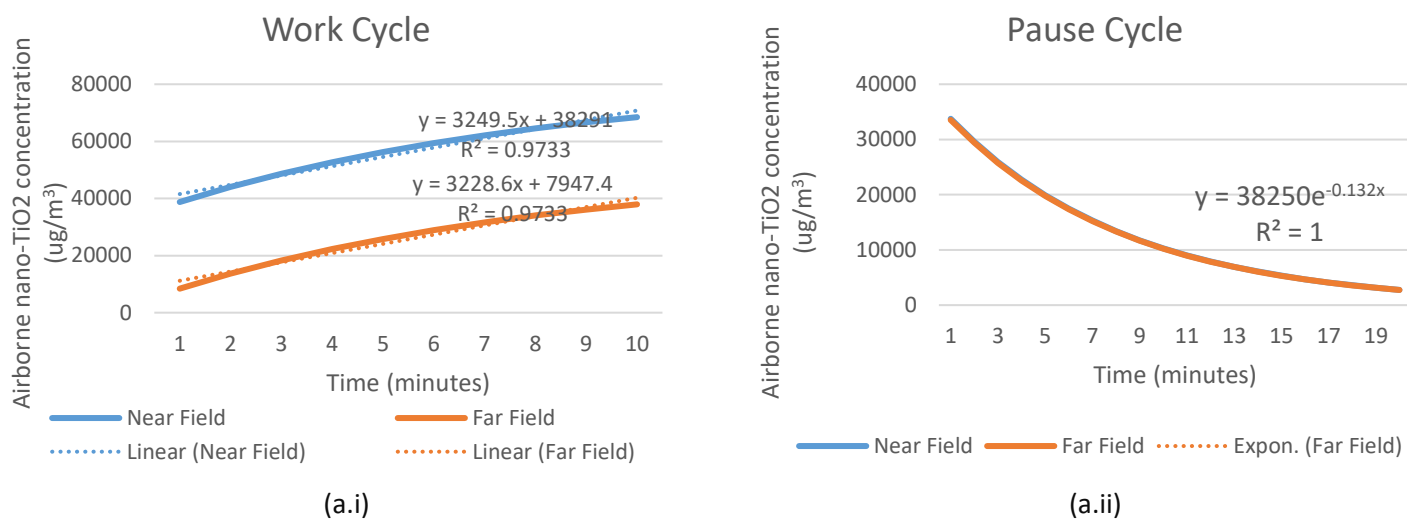
Supporting Information

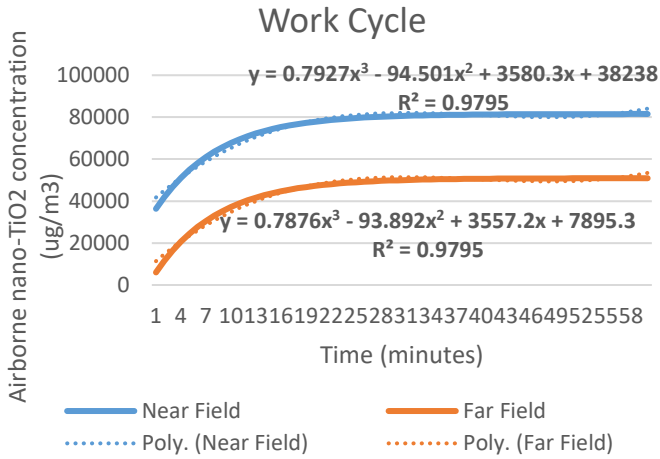
Michael P. Tsang,^{1,2} Dingsheng Li,^{3,4} Kendra L. Garner,^{3,4} Arturo A. Keller,^{3,4} Sangwon Suh,^{3,4} Guido W. Sonnemann^{1,2*}

1. Univ. Bordeaux, ISM, UMR 5255, F-33400 Talence, France
2. CNRS, ISM, UMR 5255, F-33400 Talence, France
3. Bren School of Environmental Science & Management, University of California, Santa Barbara, CA 93106-5131, USA
4. University of California, Center for Environmental Implications of Nanotechnology (UC CEIN), Santa Barbara, CA, USA

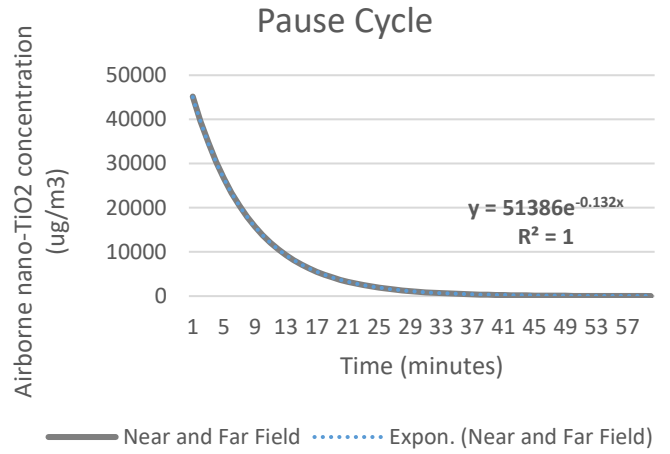
*Corresponding Author: guido.sonnemann@u-bordeaux.fr

Results of the fate and transport model are shown in **Figure S1** for the six different exposure scenarios assessed in this study. Emissions are shown for the near-field and far-field indoor air compartments during the emission event and during periods of rest (where applicable).

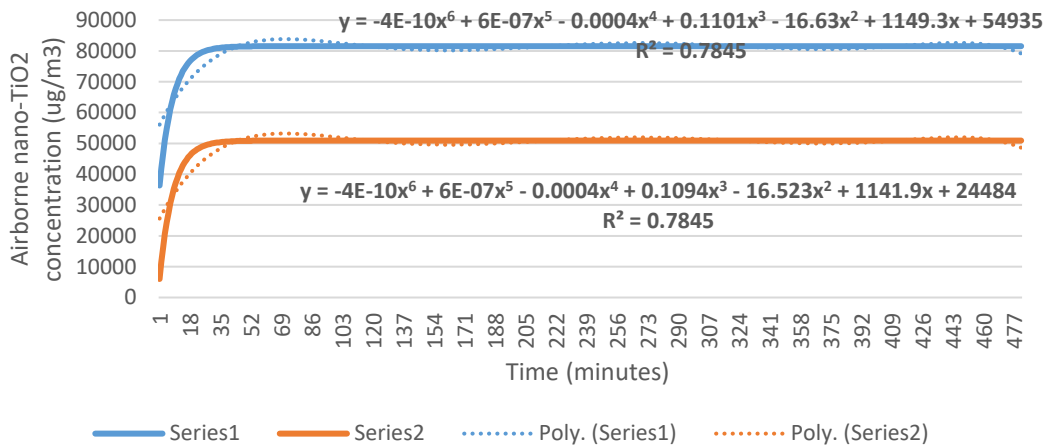




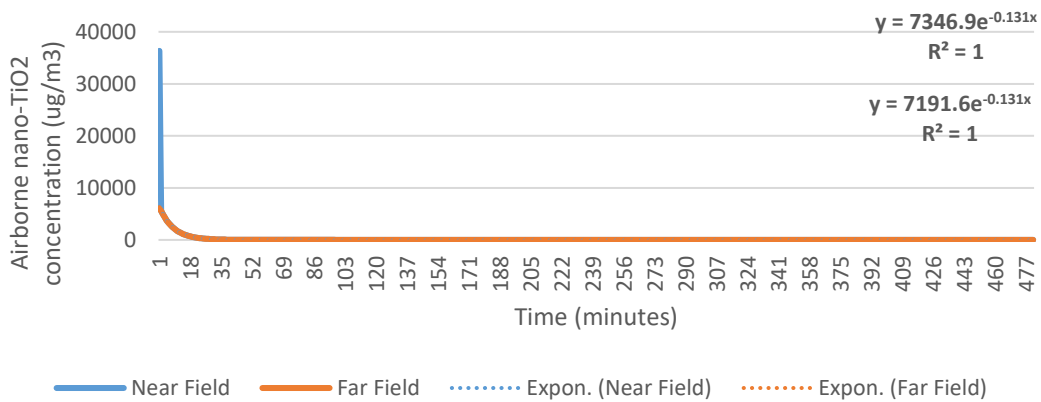
(b.i)



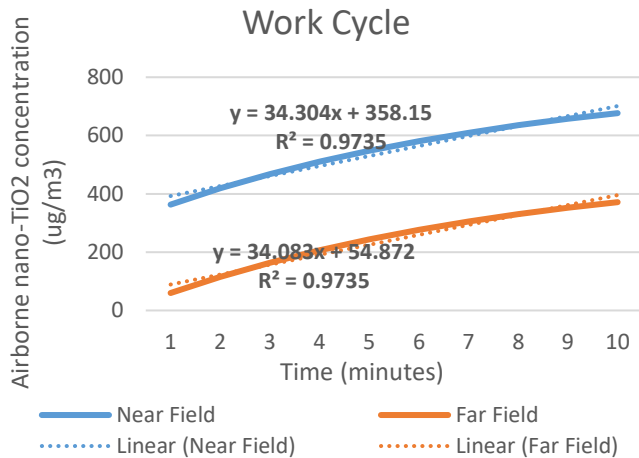
(b.ii)



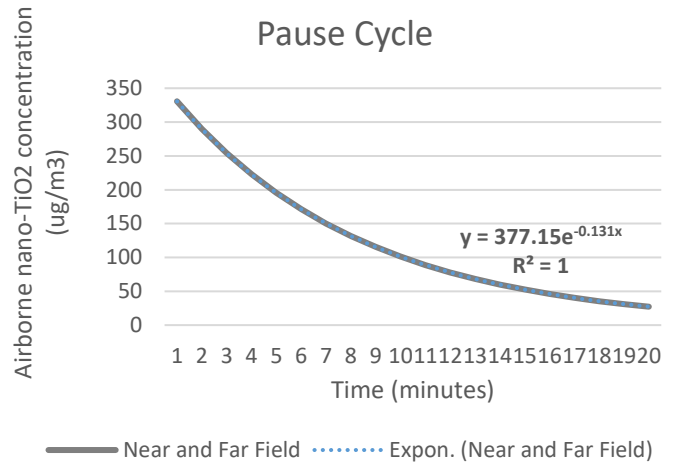
(c.i)



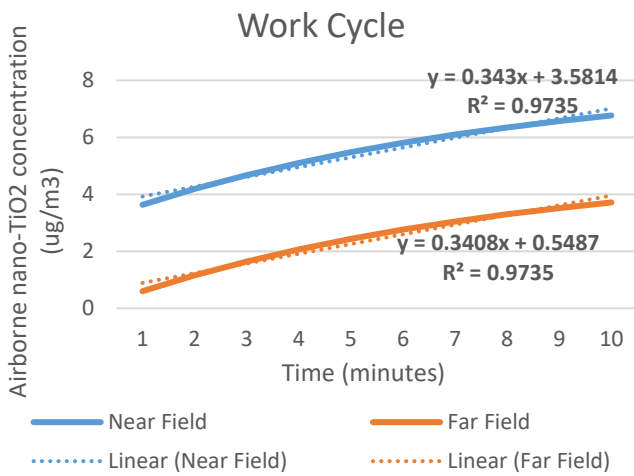
(c.ii)



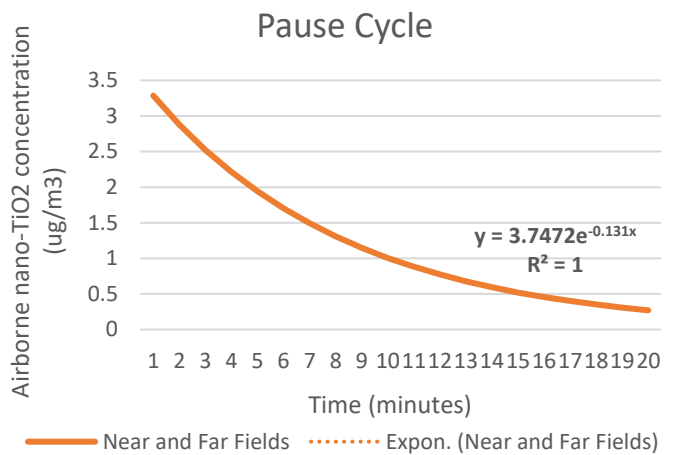
(d.i)



(d.ii)



(e.i)



(e.ii)

Figure S1 Trends in the airborne nano-TiO₂ concentrations for ES1-ES6 corresponding with rows a-e and during work cycles (i) and non work cycles (ii).

Parameters and their values used to run the MPPD deposition model.

Table S1 Inputs to the Multiple-Path Particle Dosimetry (MPPD) v3.01 model

Parameter	Value	Units	Source
Model Mode	Deposition Only	--	--
Species	Human	--	--
Model	Symmetric	--	--
Functional residual capacity	3300	ml	(Default MPPD value)
Upper Respiratory Tract Volume	50	ml	(Default MPPD value)
Aerosol (Particle) Concentration	54.28	mg/m ³	*
Breathing Frequency	17.5	min ⁻¹	1
Tidal Volume	1143	ml	1
Inspiratory Fraction	0.5	%	(Default MPPD value)
Pause Fraction	0.0	%	N/A
Breathing Scenario	Nasal	--	--
Gravity Acceleration	981	cm/s ²	--
Particle Density	3.9	g/cm ³	2
Aspect Ratio	1	--	A value of 1 correlates with perfectly spherical particles

Diameter	0.0210	μm	--
GSD	1	--	(Default MPPD value)

* The average reported ENM concentration during a given work cycle, once a pseudo-steady-state environmental concentration was seen, was used as input into the MPPD model.

An inhalation rate of 34 L/min was assumed during the work-related activity, while it decreased to 14 L/min during non-work activities.³ Blood flow was modeled considering heavy exercise during the 8-hour workday, for 5 workdays per week, while non-working hours and non-workdays reflected blood flow values for people at rest.

The parameters used in the PBPK model are displayed in **Table S2**.

Table S2 Parameters and their values for operating the PBPK exposure model. These parameters are part of a larger model and set of code that is available upon request.

ENM-specific Parameters	
CLEu = 0.0543	clearance rate to urine from blood in kidneys, Li et al., 2016 - 1/min
CLEf = 2.53e-4	clearance rate to feces from liver, Li et al., 2016 - 1/min
CLEf _{GI} = 2.35e-3	clearance rate to feces from GI tract, Li et al., 2016 - 1/min
ku _{agi} = 5.58e-3	clearance rate from upper airway region, Li et al., 2016 - 1/min
k _{ab0} = 18.8	maximum uptake rate by phagocytizing cells, Carlander et al., 2016 - 1/min
k _{sab0} = 0.126	maximum uptake rate by phagocytizing cells in spleen, Carlander et al., 2016 - 1/min
k _{de} = 8.83e-21	desorption rate by phagocytizing cells, Li et al., 2016 - 1/min
ku _{abr} = 1.39e-6	transport factor from upper airway region to brain via the olfactory bulb, Li et al., 2016 - 1/min
k _{pulmtra} = 1.44e-6	transport factor from inactive pulmonary phagocytizing cells to tracheobronchial region, Li et al., 2016 - 1/min
k _{tragi} = 9.2e-5	transport factor from tracheobronchial region to GI tract, Li et al., 2016 - 1/min
k _{giab} = 9.02e-5	absorption rate of GI tract, Li et al., 2016 - 1/min
k _{luip} = 1.87e-8	transfer rate from interstitium of lungs to pulmonary region, Li et al., 2016 - 1/min
k _{lupi} = 2.1e-3	transfer rate from pulmonary region to interstitium of lungs, Li et al., 2016 - 1/min
M _{cap} = 1.21e-6	maximum uptake capacity in individual phagocytizing cells, Carlander et al., 2016 - ug
N _{bloodcap} = 0.185*1e+4	number of phagocytizing cells per gram blood weight, Carlander et al., 2016 - 1/g
N _{scap} = 2.08*1e+8	number of phagocytizing cells per gram immunology organs weight, Carlander et al., 2016 - 1/g
N _{lcap} = 2.72*1e+7	number of phagocytizing cells per gram liver weight, Carlander et al., 2016 - 1/g
N _{lucap} = 2.69*1e+6	number of phagocytizing cells per gram lungs weight, Carlander et al., 2016 - 1/g
N _{brcap} = 3.06*1e+5	number of phagocytizing cells per gram brain weight, Carlander et al., 2016 - 1/g
N _{hcap} = 0.076*1e+6	number of phagocytizing cells per gram heart weight, Carlander et al., 2016 - 1/g
N _{kcap} = 0.99*1e+5	number of phagocytizing cells per gram kidneys weight, Carlander et al., 2016 - 1/g
N _{restcap} = 8.11*1e+6	number of phagocytizing cells per slowly perfused tissue weight, Carlander et al., 2016 - 1/g
N _{pulcap} = 3.90*1e+6	number of phagocytizing cells per pulmonary weight, Li et al., 2016 - 1/g
N _{gicap} = 0.506*1e+6	number of phagocytizing cells per GIT weight, Li et al., 2016 - 1/g
M _{bloodcap} = M _{cap} * N _{bloodcap}	maximum uptake capacity in phagocytic cells per blood weight - ug/g
M _{scap} = M _{cap} * N _{scap}	maximum uptake capacity in phagocytic cells per spleen weight - ug/g
M _{lcap} = M _{cap} * N _{lcap}	maximum uptake capacity in phagocytic cells per liver weight - ug/g
M _{lucap} = M _{cap} * N _{lucap}	maximum uptake capacity in phagocytic cells per lung weight - ug/g
M _{brcap} = M _{cap} * N _{brcap}	maximum uptake capacity in phagocytic cells per brain weight - ug/g
M _{hcap} = M _{cap} * N _{hcap}	maximum uptake capacity in phagocytic cells per heart weight - ug/g
M _{kcap} = M _{cap} * N _{kcap}	maximum uptake capacity in phagocytic cells per kidney weight - ug/g
M _{restcap} = M _{cap} * N _{restcap}	maximum uptake capacity in phagocytic cells per carcass weight - ug/g
M _{pulcap} = M _{cap} * N _{pulcap}	maximum uptake capacity in phagocytic cells per pulmonary weight - ug/g
M _{gicap} = M _{cap} * N _{gicap}	maximum uptake capacity in phagocytic cells per GIT weight - ug/g
P = 0.974	partition coefficient tissue:blood, Carlander et al., 2016 - unitless
X _{rich} = 0.126	permeability coefficient from blood to richly perfused tissue, Carlander et al., 2016 - unitless
X _{br} = 1.92e-6	permeability coefficient from blood to brain tissue, Carlander et al., 2016 - unitless
X _{rest} = 2.13e-5	permeability coefficient from blood to rest of the body, Carlander et al., 2016 - unitless

frbr=0.371
 fro=0.144
 delaygi = 112.8
 delayf = 474

fraction of capillary blood remained in brain when measured, Li et al., 2016 - unitless
 fraction of capillary blood remained in other organs when measured, Li et al., 2016 - unitless
 time delay for nanoparticles to travel from respiratory system to GI tract, Li et al., 2016 - min
 time delay for nanoparticles in feces be excreted out, Li et al., 2016 - min

Human physiologic parameters

BW = 75000	body weight for workers, assumption of higher % of male in this specific workforce - g
Qtot = IF work=1 THEN 25000 ELSE 5000	cardiac output, heavy excercise, literature - mL/min
Ws = 169.25	weight of spleen, literature - g
Wgi = 2265	weight of GI tract, literature - g
Wl = 1463.5	weight of liver, literature - g
Wlu = 984	weight of lungs, literature - g
Wbr = 1342.9	weight of brain, literature - g
Wh = 288.6	weight of heart, literature - g
Wk = 314.375	weight of kidneys, - g
Wblood = Wbloodt-Wsb-Wgib-Wlb	weight of arterial and venous blood, literature - g
Wbloodt = 0.07*BW	weight of total blood, literature - g
Wrest = BW-Ws-Wgi-Wl-Wlu-Wbr-Wh-Wk-Wbloodt	weight of rest of the body, literature - g
Wsb = 0.22*Ws	weight of blood in spleen, from literatures for rat - g
Wgib = 0.1*Wgi	weight of blood in GI tract, estimated - g
Wlb = 0.21*Wl	weight of blood in liver, from literatures for rat - g
Wlub = 0.36*Wlu	weight of blood in lungs, estimated - g
Wbrb = 0.03*Wbr	weight of blood in brain, values from literatures for rat - g
Whb = 0.26*Wh	weight of blood in heart, values from literatures for rat - g
Wkb = 0.16*Wk	weight of blood in kidneys, values from literatures for rat - g
Wrestb = 0.017*Wrest	weight of blood in rest of the body, values from literatures for rat - g
fQs = 0.03	fraction of cardiac output to spleen, literature - unitless
fQgi = IF workingday*workinghour=1 THEN 0.05 ELSE 0.2	fraction of cardiac output to GI tract, literature - unitless
fQl = IF workingday*workinghour=1 THEN 0.11 ELSE 0.25	fraction of cardiac output to liver, literature - unitless
fQbr = IF workingday*workinghour=1 THEN 0.04 ELSE 0.15	fraction of cardiac output to brain, literature - unitless
fQh = 0.05	fraction of cardiac output to heart, literature - unitless
fQk = IF workingday*workinghour=1 THEN 0.04 ELSE 0.20	fraction of cardiac output to kidneys, literature - unitless
fQrest = 1-fQs-fQgi-fQl-fQbr-fQh-fQk	fraction of cardiac output to rest of the body, literature - unitless
Qs = fQs*Qtot	blood flow to spleen - mL/min
Qgi = fQgi*Qtot	blood flow to GI tract - mL/min
Ql = fQl*Qtot	blood flow to liver - mL/min
Qbr = fQbr*Qtot	blood flow to brain - mL/min
Qh = fQh*Qtot	blood flow to heart - mL/min
Qk = fQk*Qtot	blood flow to kidneys - mL/min
Qrest = fQrest*Qtot	blood flow to rest of the body - mL/min

Defining the Effect Factor (EF) and Does-response Modeling

The dose response data used to estimate the ED50 carcinogenic and non-carcinogenic data are displayed in **Table S3** and **Table S4**.

Table S3 Toxicological data used to calculate the carcinogenic dose-response relationship

Concentration mg/m3	Dose mg/g-dry lung	Dose m ² /dry lung	Dose m ² /g-dry lung	Animal Gender	Animal Sample Size	Species	Cancer Cases	References
0	0.00	0.00	0.00	F	77	R	2	Lee et al. ¹³
10	32.30	0.16	0.07	F	75	R	2	Lee et al. ¹³

50	130.00	0.65	0.28	F	74	R	1	Lee et al. ¹³
250	545.80	2.72	1.16	F	74	R	12	Lee et al. ¹³
0	0.00	0.00	0.00	M	79	R	2	Lee et al. ¹³
10	20.70	0.10	0.03	M	71	R	2	Lee et al. ¹³
50	118.30	0.59	0.18	M	75	R	1	Lee et al. ¹³
250	784.80	3.92	1.20	M	77	R	12	Lee et al. ¹³
0	0	0.00	0.00	MF	100	R	3	Muhle et al. ¹²
5	2.72	0.01	0.01	MF	100	R	2	Muhle et al. ¹²
0	0	0.00	0.00	F	217	R	1	Heinrich et al. ¹⁵
10	39.29	1.89	1.31	F	100	R	32	Heinrich et al. ¹⁵

Table S4 Toxicological data used to calculate the non-carcinogenic dose-response data¹⁰

Dose mg/m3	Dose µg/g-dry lung	Diameter (nm)	Species	BAL Cell Sample Size	Macrophages (%)	Macrophages (Count)	Neutrophil (%)	Neutrophil (Count)
0	5.71	21	M	200	0.99	198	0	0
0	21.0	21	M	200	1	200	0	0
0	14.1	21	M	200	0.99	198	0	0
0	32.7	21	M	200	1	200	0	0
0	15.5	21	M	200	1	200	0	0
0.5	381	21	M	200	0.995	199	0	0
0.5	335	21	M	200	1	200	0	0
0.5	349	21	M	200	0.995	199	0	0
0.5	361	21	M	200	0.99	198	0	0
0.5	365	21	M	200	1	200	0	0
2	1411	21	M	200	0.995	199	0.005	1
2	1458	21	M	200	1	200	0	0
2	1411	21	M	200	1	200	0	0
2	1400	21	M	200	0.995	199	0.005	1
2	1299	21	M	200	1	200	0	0
10	10860	21	M	200	0.8	160	0.195	39
10	9776	21	M	200	0.865	173	0.125	25
10	11080	21	M	200	0.915	183	0.07	14
10	10306	21	M	200	0.775	155	0.21	42
10	10540	21	M	200	0.875	175	0.125	25
0	42.4	21	R	200	1	200	0	0
0	35.3	21	R	200	0.995	199	0.005	1
0	35.5	21	R	200	1	200	0	0
0	38.6	21	R	200	0.99	198	0.01	2
0	31.4	21	R	200	0.99	198	0.005	1
0.5	423	21	R	200	0.995	199	0.005	1
0.5	454	21	R	200	0.985	197	0.01	2
0.5	483	21	R	200	0.99	198	0.005	1
0.5	382	21	R	200	0.99	198	0.005	1
0.5	380	21	R	200	1	200	0	0
2	1620	21	R	200	0.91	182	0.085	17
2	1769	21	R	200	0.97	194	0.03	6
2	1772	21	R	200	0.96	192	0.035	7
2	1605	21	R	200	0.87	174	0.13	26
2	1660	21	R	200	0.95	190	0.045	9
10	10211	21	R	200	0.235	47	0.73	146
10	12383	21	R	200	0.4	80	0.585	117
10	10110	21	R	200	0.365	73	0.625	125
10	11440	21	R	200	0.315	63	0.66	132
10	10793	21	R	200	0.35	70	0.64	128

Estimations of particle deposition in the lung as estimated by the MPPD model are displayed in **Figure S2**.

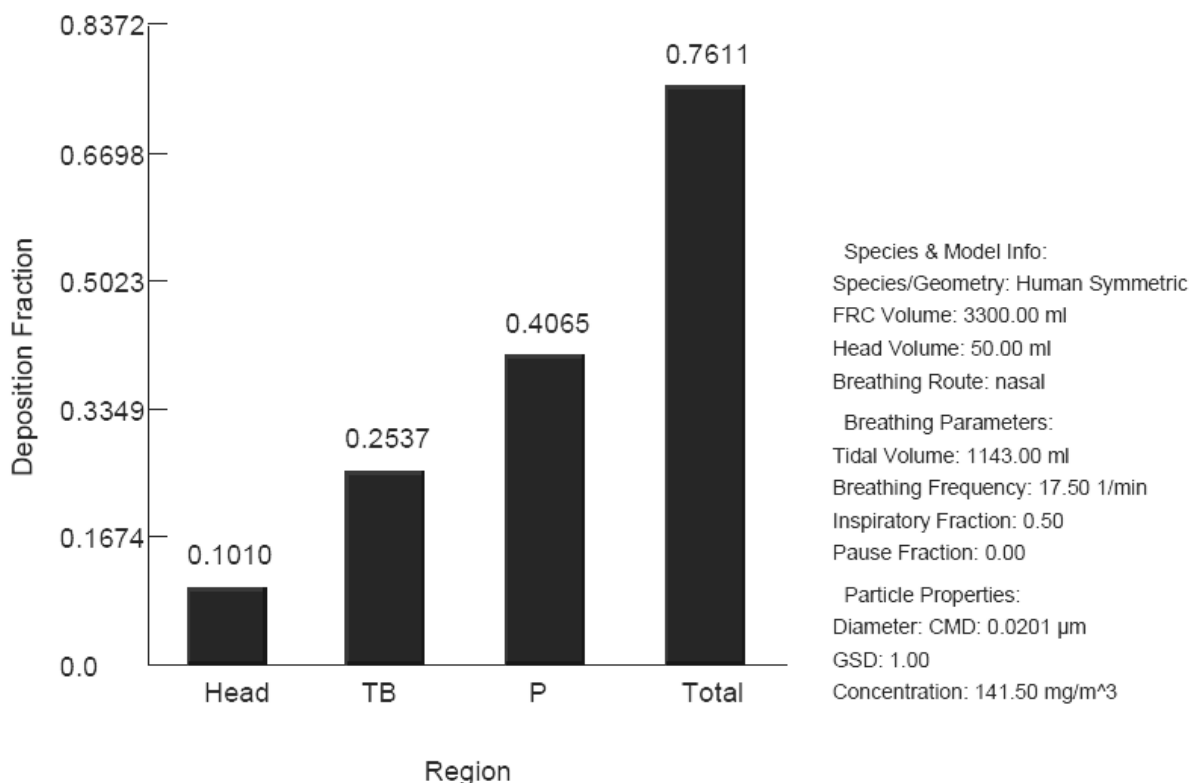


Figure S2 Deposition of the 21 nm nano-TiO₂ in the human lung as calculated using the MPPD model

Exposure Results

ES1 e-high, f-short

The retention in the trachea-bronchial region was similar to the retention pattern in the wet lung, whereby accumulation quickly increased and then leveled off by the 5th work-week. Its maximum retention was only 12% lower than the wet lung's value and thus represents an important consideration in the overall exposure since ENM in this region can be transferred to other organ systems such as the gut. Comparatively, accumulation in the upper airway (i.e. head, nasal regions) was less significant. The upper airway cleared all nano-TiO₂ by each subsequent workday. The maximum retention in this region by the end of the first work-year was 9.80E+03 µg, over 1-order of magnitude smaller than the retention of the wet lung.

ES2 e-high, f-long

Over the course of 1-work day the wet lung burden increased 6 different times, corresponding with each of the 6 work-cycles and emission events. Between work cycles, exposures increased very slightly. At the end of the first workday, there was a maximum wet lung burden of 223 µg/g-wet lung. The lung burden did not decrease sufficiently between workdays or workweeks to clear the lung of its total nano-TiO₂ load. For example, the maximum exposure by the end of the first work-week was 656 µg/g-wet lung, while at the start of the second work-week it was 475 µg/g-wet lung. This trend continued until the 6th work-week, after which maximum weekly accumulations slowed considerably, having already reached 917 µg/g-wet lung which is 94% of the maximum lung burden of 980 µg/g-wet lung at the end of the year (**Figure S3**).

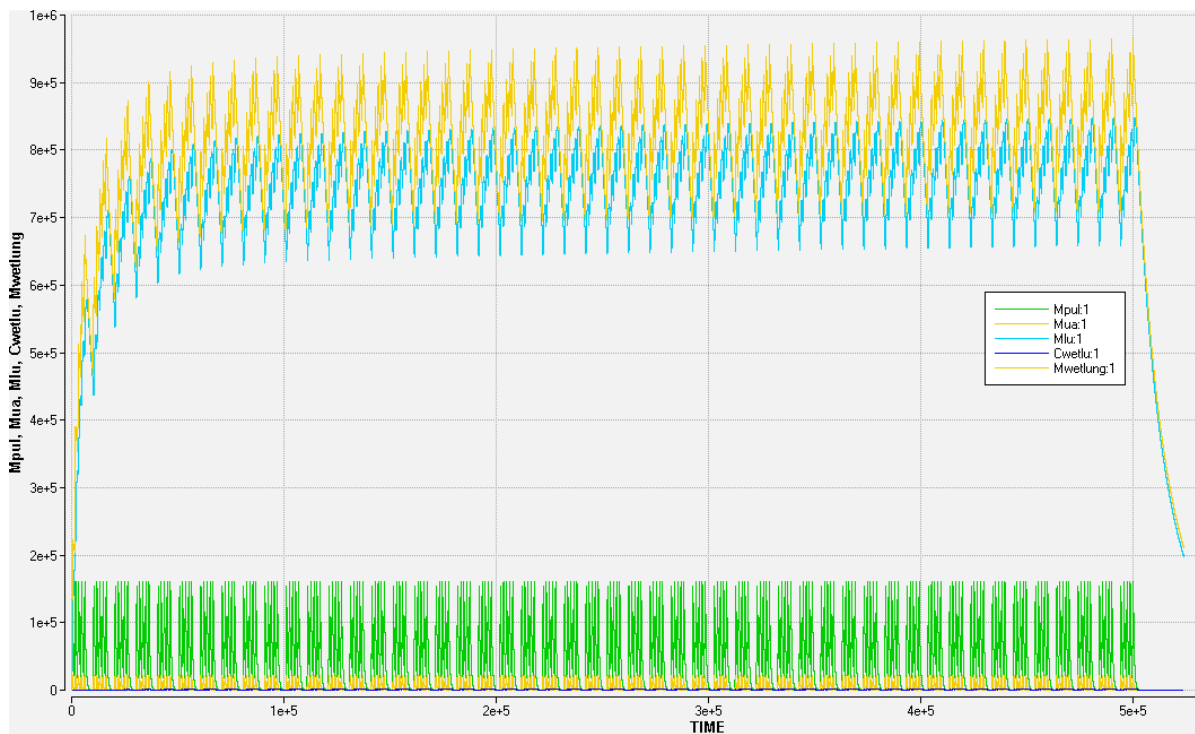


Figure S3 Retention of nano-TiO₂ in the lung estimated over 1 full work year for ES2. The x-axis represents time in minutes over 1-year and the y-axis represents the mass (μg) of nano-TiO₂ in the wet lung. The green trend line represents the change in mass in the air-exchange (pulmonary) regions of the lung, the blue trend line represents the change in mass in the interstitial regions of the lung, the pink trend line represents the change in mass in the trachea-bronchial regions of the lung, the red trend line represents the total retention in the wet lung including the air-exchange (pulmonary) regions, interstitial regions, trachea-bronchial regions and their macrophages.

The 1-year time-weighted lung burden over a lifetime was $11.6 \mu\text{g/g}$ -wet lung, and the lifetime lung-burden was $553 \mu\text{g/g}$ -wet lung. The corresponding 1-year and lifetime RiF values were $3.55\text{E-}11$ and $1.69\text{E-}09$, respectively.

Lung burden was mainly influenced by the retention of nano-TiO₂ in the interstitial region, where it represented up to 81% of the retained wet lung mass by the end of the first work-year. In contrast, the pulmonary region cleared itself of all deposited nano-TiO₂ by the beginning of each subsequent work-week. Even so, the pulmonary region contributed up to 17% of the total maximum retention observed each day by the end of the first work-year. The PC located in the interstitial and pulmonary regions reached maximum retentions of $3202 \mu\text{g}$ and $4644 \mu\text{g}$, respectively, very quickly within the first workday. This represented roughly 0.3% and 0.5% of the total lung burden by the end of the first work-year.

Retention in the trachea-bronchial region was similar to the retention pattern in the wet lung, whereby accumulation quickly increased and then leveled off by the 6th work-week. Its maximum retention was 10% lower than the wet lung's maximum retention value and thus represents an important consideration in the overall exposure as explained previously for ES1. Comparatively, accumulation in the upper airway was less significant. The upper airway cleared all nano-TiO₂ after each subsequent workday. The maximum

retention in this region by the end of the first work-year was $2.2\text{E}+04 \mu\text{g}$, over 1-order of magnitude smaller than retention in the wet lung.

ES3 e-high, f-daily

Over the course of 1-work day the wet lung burden increased steadily without pause and correlated with the all-day, constant exposure emissions of this model. At the end of the first workday, the maximum lung burden was $486 \mu\text{g/g-wet lung}$. The lung burden did not decrease sufficiently between workdays or workweeks (i.e. over the weekends) to clear the lung of its total nano-TiO₂ load. For example, the maximum exposure by the end of the first work-week was $1.45\text{E}+03 \mu\text{g/g-wet lung}$, while at the beginning of the second work-week it was $1.02\text{E}+03 \mu\text{g/g-wet lung}$. This trend continued until the 6th work-week, after which maximum weekly accumulations slowed considerably, having already reached $1.99\text{E}+03 \mu\text{g/g-wet lung}$ which is 96% of the maximum lung burden of $2.08\text{E}+03 \mu\text{g/g-wet lung}$ at the end of the year (Figure S4).

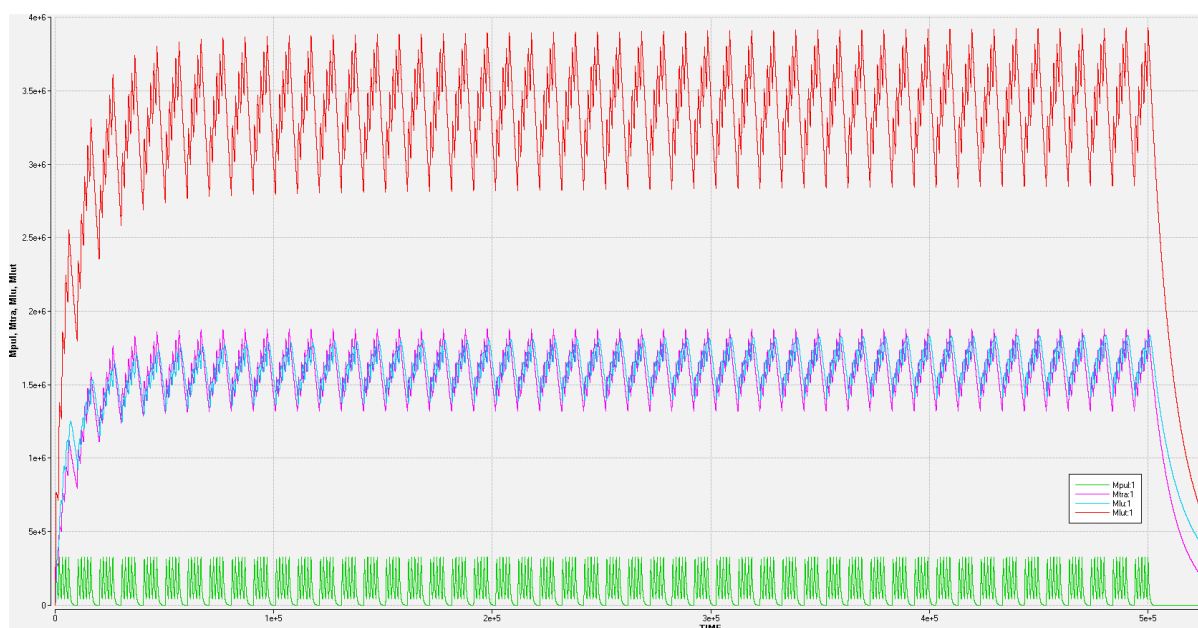


Figure S4 Retention of nano-TiO₂ in the lung estimated over 1 full work year for ES3. The x-axis represents time in minutes over 1-year and the y-axis represents the mass (μg) of nano-TiO₂ in the wet lung. The green trend line represents the change in mass in the air-exchange (pulmonary) regions of the lung, the blue trend line represents the change in mass in the interstitial regions of the lung, the pink trend line represents the change in mass in the trachea-bronchial regions of the lung, the red trend line represents the total retention in the wet lung including the air-exchange (pulmonary) regions, interstitial regions, trachea-bronchial regions and their macrophages.

A two-week period of non-work activity (i.e. assumed standard holiday) between work years was assumed. The 1-year time-weighted lung burden over a lifetime was $25 \mu\text{g/g-wet lung}$, and the lifetime lung-burden was $1.19\text{E}+03 \mu\text{g/g-wet lung}$. The corresponding 1-year and lifetime RiF values were $3.82\text{E}-11$ and $1.82\text{E}-09$, respectively.

Lung burden was mainly influenced by the retention of nano-TiO₂ in the interstitial region, where it represented up to 90% of the retained wet lung mass by the end of the first work-year. In contrast, the pulmonary region cleared itself of all deposited nano-TiO₂ by the beginning of each subsequent work-week. Even so, the pulmonary region contributed up to 16% of the total maximum retention observed

each day by the end of the first work-year. The PC located in the interstitial and pulmonary regions reached maximum retentions of 3202 µg and 4644 µg, respectively, very quickly within the first workday. This represented roughly 0.20% and 0.23% of the total lung burden by the end of the work-year.

Retention in the trachea-bronchial region was similar to the retention pattern in the wet lung, whereby accumulation quickly increased and then leveled off by the 6th work-week. Its maximum retention was only 8% lower than the wet lung's maximum retention value and thus represents an important consideration in the overall exposure as explained previously for ES1. Comparatively, accumulation in the upper airway was less significant. The upper airway cleared all nano-TiO₂ by each subsequent workday. The maximum retention in this region by the end of the first work-year was 4.1E+04 µg, over 1-order of magnitude smaller than retention in the wet lung.

ES4 e-high, f-single pulse

Over the course of 1-work day there was an initial maximum daily lung burden seen within the first hour of exposure, which then slightly decreased by the end of the workday to 0.72 µg/g-wet lung. There were no decreases between workdays nor was there significant decreases between workweeks. This trend continued until the 18th work-week when there was a sudden spike in total wet lung retention. The peak of this increase occurred at week 21, reaching 12.4 µg-g-wet lung, but then receded to approximately 11.1 µg/g-wet lung by week 25. Thereon, the maximum wet lung retention stayed consistent around 11.1 µg/g-wet lung until the end of the year ().

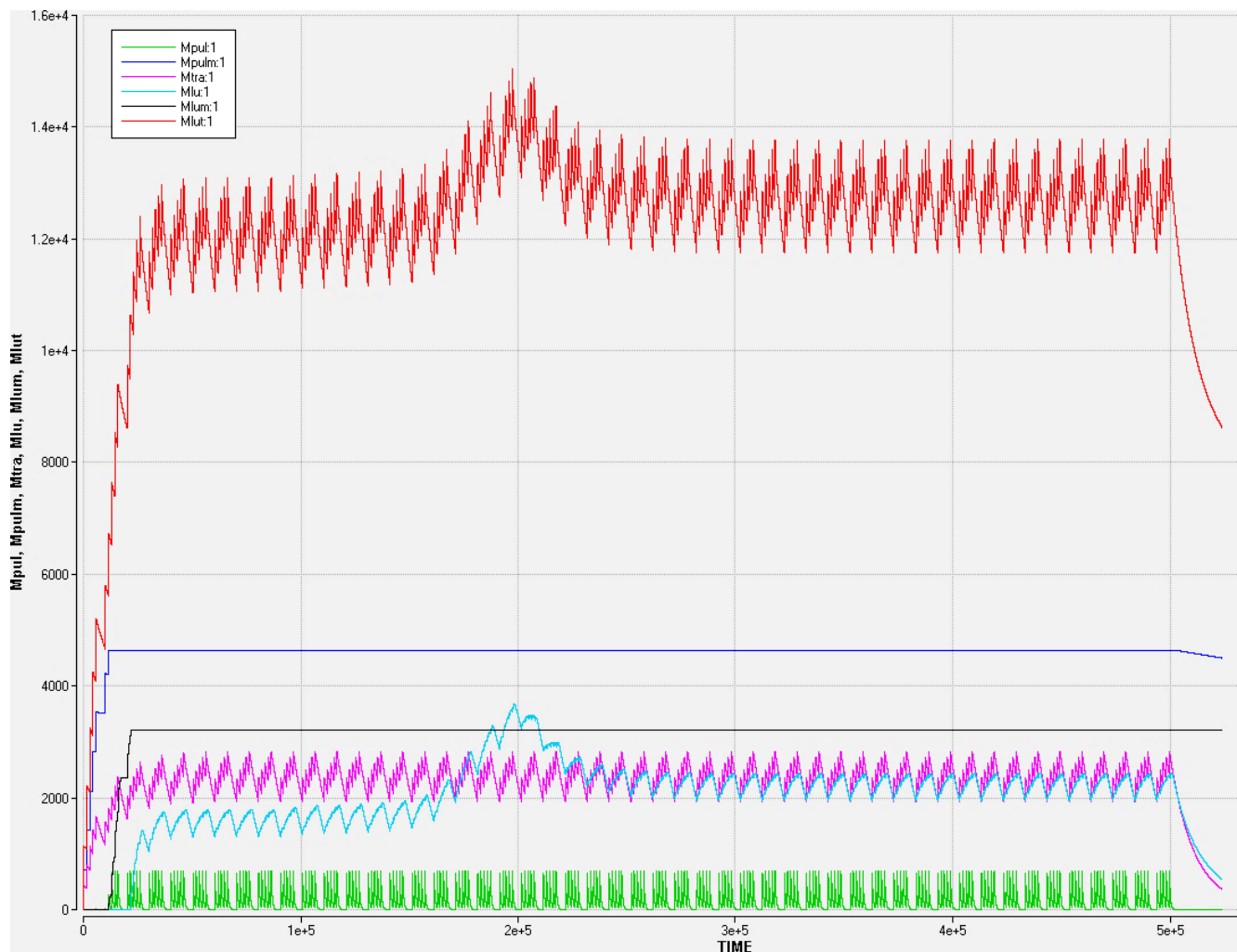


Figure S5 Retention of nano-TiO₂ in the lung estimated over 1 full work year for ES4. The x-axis represents time in minutes over 1-year and the y-axis represents the mass (μg) of nano-TiO₂ in the wet lung. The green trend line represents the change in mass in the air-exchange (pulmonary) regions of the lung, the blue trend line represents the change in mass in the interstitial regions of the lung, the pink trend line represents the change in mass in the trachea-bronchial regions of the lung, the grey trend line represents the change in mass in the lung macrophages, the dark-blue line represents the change in mass in the pulmonary macrophages, the red trend line represents the total retention in the wet lung including the air-exchange (pulmonary) regions, interstitial regions, trachea-bronchial regions and their macrophages.

The 1-year time-weighted lung burden over a lifetime was $0.14 \mu\text{g/g-wet lung}$, and the lifetime lung-burden was $7.04 \mu\text{g/g-wet lung}$. The corresponding 1-year and lifetime RiF values were $1.05\text{E-}10$ and $5.16\text{E-}09$, respectively.

Lung burden was mainly influenced by the retention of nano-TiO₂ in the interstitial and pulmonary PC, where they represented 29% and 42%, respectively, of the maximum retained dose seen at the end of the year (**Figure S5**). The interstitium had a maximum retention of $3.20\text{E}+03 \mu\text{g}$ by the end of the work year. This was 22% of the total wet lung retention and contrasts with ES1-ES3 where the interstitium was the most significant contributor to the total wet lung burden. The pulmonary region cleared itself of all deposited nano-TiO₂ by the beginning of each subsequent work-week. This region only contributed up to 6% of the maximum wet lung retention observed at the end of the first work-year.

Retention in the trachea-bronchial region was similar to the retention pattern in the wet lung, however there was no secondary spike in this region's retention, which had leveled off by the 5th work-week. Its maximum retention was 74% lower than the wet lung's maximum retention value. Comparatively, accumulation in the upper airway was negligible and only represented 1% of the total wet lung retention by the end of the work-year.

ES5 e-medium, *f-short*

Over the course of 1-work day there were 16 distinct increases in wet lung retention that corresponded with the 16 emission events throughout the day. By the end of the first workday the maximum wet lung retention was 1.15 $\mu\text{g/g}$ -wet lung. There was little decrease between workdays and between work-days. This trend continued until the 11th work-week when there was a sudden spike in total wet lung retention. The peak of this increase occurred at week 14, reaching 14 μg -wet lung, but then receding to approximately 12.6 $\mu\text{g/g}$ -wet lung by week 17. Thereon, the maximum wet lung retention stayed consistent around 12.6 $\mu\text{g/g}$ -wet lung until the end of the work-year (Figure S6).

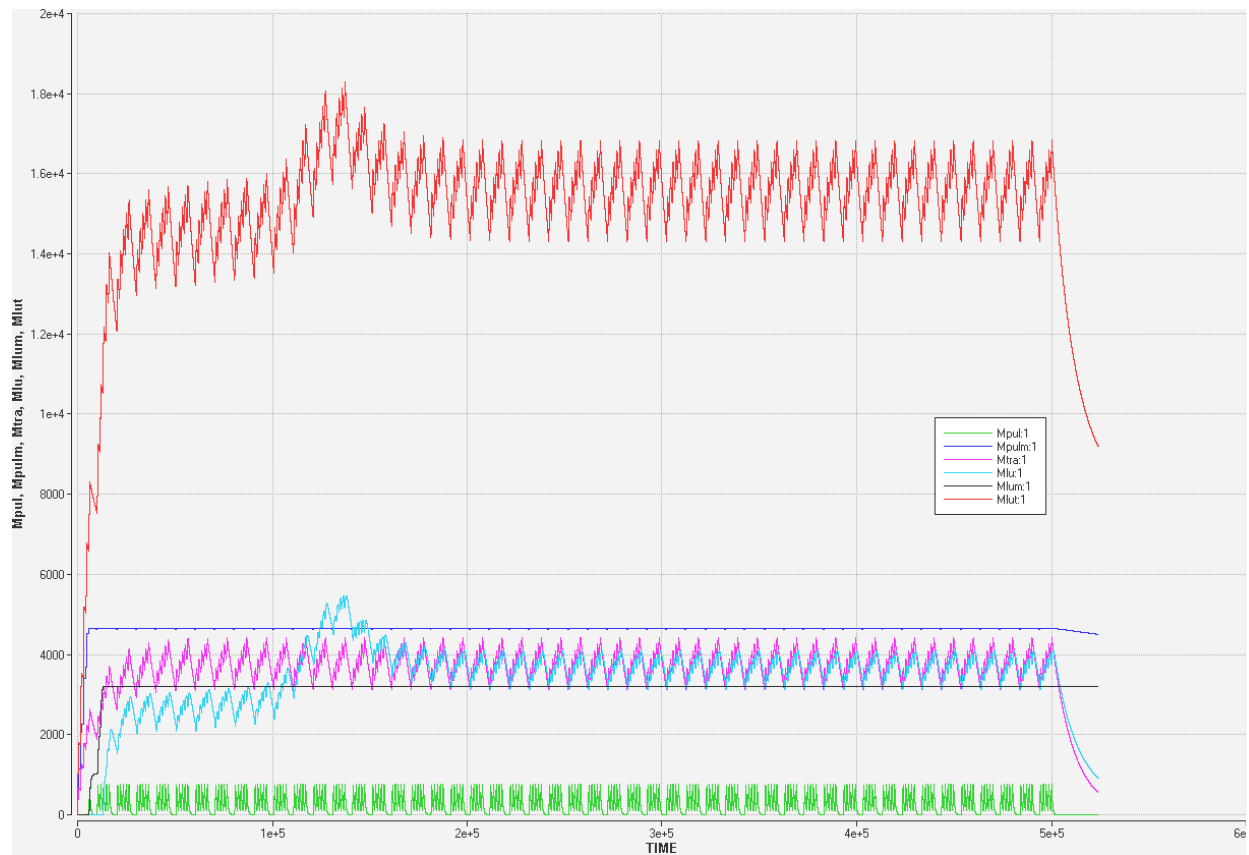


Figure S6 Retention of nano-TiO₂ in the lung estimated over 1 full work year for ES5. The x-axis represents time in minutes over 1-year and the y-axis represents the mass (μg) of nano-TiO₂ in the wet lung. The green trend line represents the change in mass in the air-exchange (pulmonary) regions of the lung, the blue trend line represents the change in mass in the interstitial regions of the lung, the pink trend line represents the change in mass in the trachea-bronchial regions of the lung, the grey trend line represents the change in mass in the lung macrophages, the dark-blue line represents the change in mass in the pulmonary macrophages, the red trend line represents the total retention in the wet lung including the air-exchange (pulmonary) regions, interstitial regions, trachea-bronchial regions and their macrophages.

The 1-year time-weighted lung burden over a lifetime was 0.17 $\mu\text{g/g}$ -wet lung, and the lifetime lung-burden was 8.10 $\mu\text{g/g}$ -wet lung. The corresponding 1-year and lifetime RiF values were 7.64E-11 and 3.17E-09, respectively.

Lung burden was mainly influenced by the retention of nano-TiO₂ in the pulmonary PC, where they accounted for 38% of the maximum total retention by the end of the work-year. The interstitium accounted for 32% of the maximum total wet lung retention and was also correlated with the rapid and steep spike in retention seen between weeks 11-17 similar to ES4. The interstitial PC contained 26% of the maximum total wet lung retention. The pulmonary and interstitial PC reached their maximum total retention by the end of the first work-week. The pulmonary region cleared itself of all deposited nano-TiO₂ by the beginning of each subsequent week. This region only contributed up to 4% of the maximum wet lung retention observed at the end of the first year.

Retention in the trachea-bronchial region was similar to the retention pattern in the wet lung, however there was no secondary spike in this region's retention, which had leveled off by the 5th work-week. Its maximum retention was 65% lower than the wet lung's maximum retention value. Comparatively, accumulation in the upper airway was negligible and only represented < 1% of the total wet lung retention by the end of the work-year.

ES6 e-low, f-short

Over the course of 1-work day there were 16 distinct increases in wet lung retention that corresponded with the 16 emission events. By the end of the first workday the maximum wet lung retention was 1.15E-02 $\mu\text{g/g}$ -wet lung. There was little decrease between workdays and between work-days. Total retention continued largely unabated, reaching a maximum total wet lung retention of 2030 $\mu\text{g/g}$ -wet lung by the end of the first work-year (**Figure S7**).

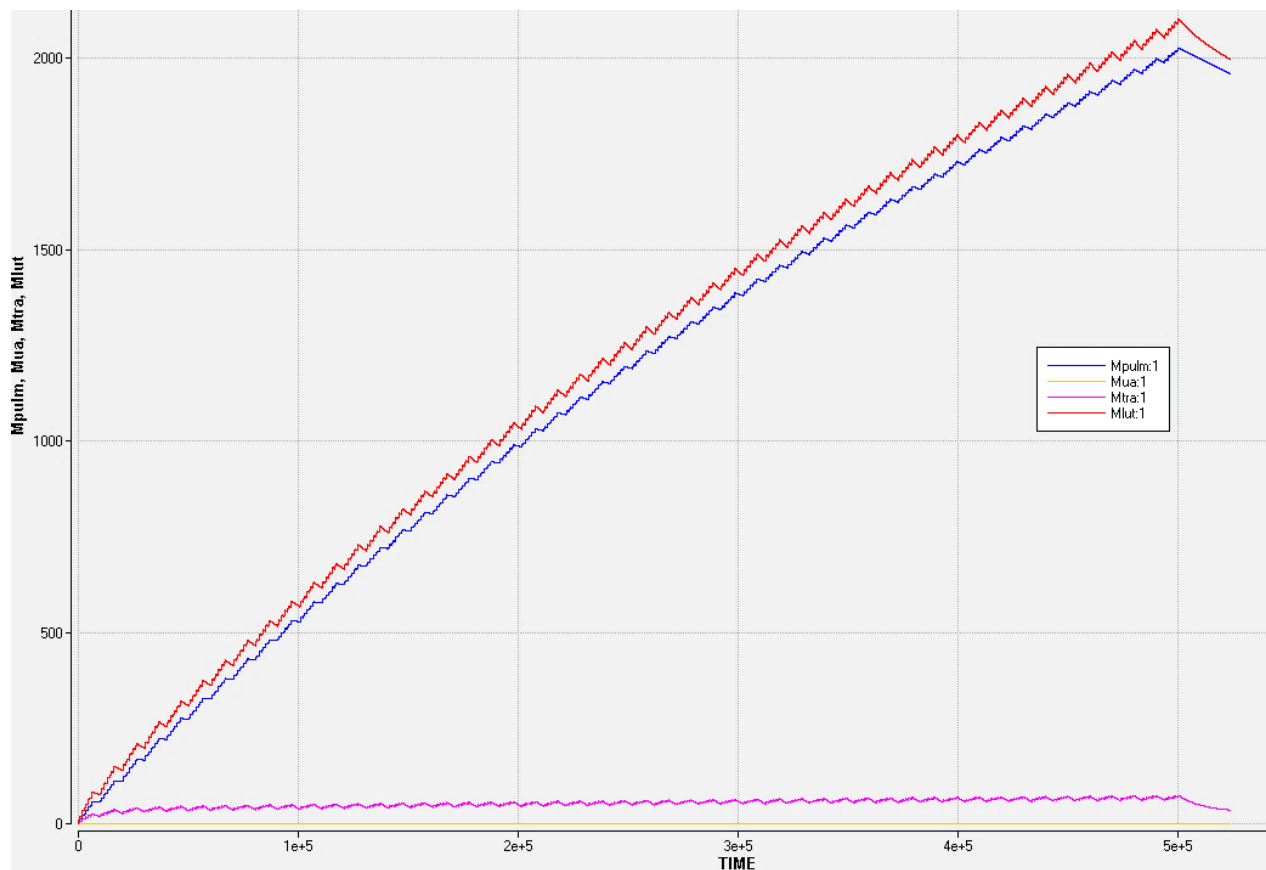


Figure S7 Retention of nano-TiO₂ in the lung estimated over 1 full work year for ES6. The x-axis represents time in minutes over 1-year and the y-axis represents the mass (µg) of nano-TiO₂ in the wet lung. The pink trend line represents the change in mass in the trachea-bronchial regions of the lung, the yellow trend line represents the change in mass in the upper airway, the dark-blue line represents the change in mass in the pulmonary macrophages, the red trend line represents the total retention in the wet lung including the air-exchange (pulmonary) regions, interstitial regions, trachea-bronchial regions and their macrophages.

The 1-year time-weighted lung burden over a lifetime was 1.70E-02 µg/g-wet lung, and the lifetime lung-burden was 3.99 µg/g-wet lung. The corresponding 1-year and lifetime RiF values were 7.81E-10 and 1.83E-07, respectively.

Lung burden was mainly influenced by the retention of nano-TiO₂ in the pulmonary PC, where they accounted for 99.9% of the maximum total retention by the end of the work-year. Retention in the trachea-bronchial region was similar to the retention pattern in the wet lung, which increased largely unabated throughout the work-year. Its maximum retention was 97% lower than the wet lung's maximum retention value. Comparatively, accumulation in the upper airway was negligible and only represented < 0.01% of the total wet lung retention by the end of the work-year.

Worker Population

The average worker population was estimated from survey-data reported by Walser et al.¹⁷ for industries associated with ENM manufacturing and handling. Thus, this dataset broadly captured the average number of workers involved with industries directly producing the ENM but also the downstream industries that integrate them into products. The number of workers in the ENM manufacturing sector was log-normally distributed with a geometric mean of 8.7 and geometric standard deviation of 2.8 (**Figure**

58). The low- and high-population workforce estimates were defined by the 5th- and 95th-percent confidence intervals, with corresponding values of 1.6 and 47.3 persons.

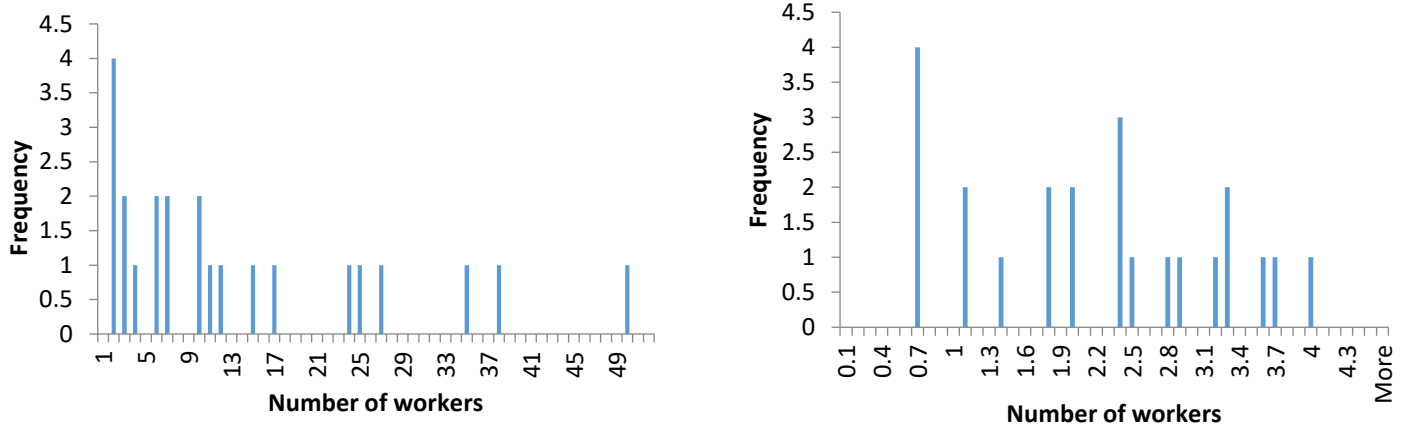


Figure S8 Number of workers along the x-axis and their frequency according to (a) original data and (b) log-transformed data presented by Walser et al.¹⁷

Relationship between the CF and emission magnitude

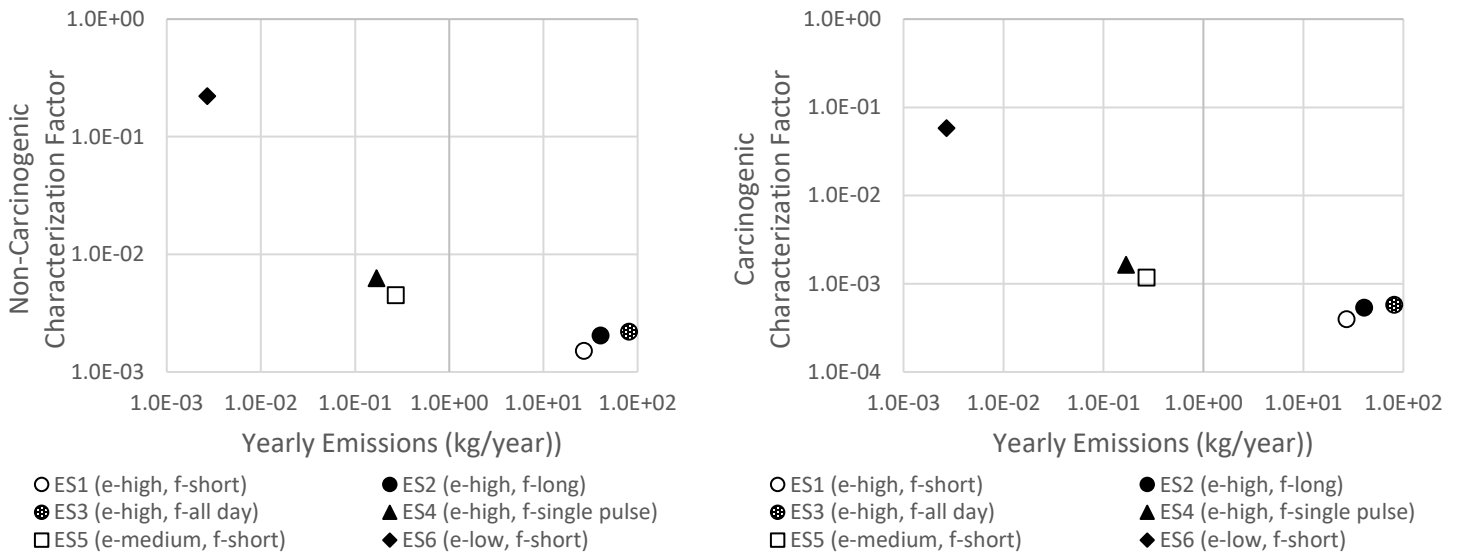


Figure S9 Non-carcinogenic characterization factors (lifetime) as a function of the total emissions per year.

Steady State Two-Zone, Near-field, Far-field Fate and Transport Equation¹⁸

$$C_{NF,eq} = \frac{S}{\left[\left(\frac{\beta}{\beta + Q}\right) \cdot Q\right] + k_i} \quad (1)$$

References

1. ICRP. *Human Respiratory Tract Model for Radiological Protection*. (1994).
2. Garner, K. L., Suh, S. & Keller, A. A. Assessing the Risk of Engineered Nanomaterials in the Environment: Development and Application of the nanoFate Model. *Environ. Sci. Technol.* **51**, 5541–5551 (2017).
3. EPA., *U. S. Exposure Factors Handbook*. (2011).
4. Jager, T., Vermeire, T. G., Rikken, M. G. J. & Van der Poel, P. Opportunities for a probabilistic risk assessment of chemicals

- in the European Union. *Chemosphere* **43**, 257–264 (2001).
5. Davis, J. A., Gift, J. S. & Zhao, Q. J. Introduction to benchmark dose methods and U.S. EPA's benchmark dose software (BMDS) version 2.1.1. *Toxicol. Appl. Pharmacol.* **254**, 181–191 (2011).
 6. Crump, K. S. A New Method for Determining Allowable Daily Intakes. *Fundam. Appl. Toxicol.* **871**, 854–871 (1984).
 7. Barlow, S. *et al.* Guidance of the scientific committee on a request from EFSA on the use of the benchmark dose approach in risk assessment. *EFSA J.* **1150**, 1–72 (2009).
 8. Crump, K. S. Calculation of Benchmark Doses from Continuous Data. *Risk Anal.* **15**, 79–89 (1995).
 9. Allen, B. C., Kavlock, R. J., Kimmel, C. a. & Faustman, E. M. Dose-response assessment for developmental toxicity: II. Comparison of generic benchmark dose estimates with no observed adverse effect levels. *Fundam. Appl. Toxicol.* **23**, 487–495 (1994).
 10. Bermudez, E. *et al.* Pulmonary responses of mice, rats, and hamsters to subchronic inhalation of ultrafine titanium dioxide particles. *Toxicol. Sci.* **77**, 347–357 (2004).
 11. *Risk Assessment of Chemicals: An Introduction.* (Springer Netherlands, 2007). doi:10.1007/978-1-4020-6102-8
 12. Muhle, H. *et al.* Pulmonary response to toner upon chronic inhalation exposure in rats. *Fundam. Appl. Toxicol.* **17**, 280–299 (1991).
 13. Lee, K. P., Trochimowicz, H. J. & Reinhardt, C. F. Pulmonary Response of Rats Exposed to Titanium by Inhalation for Two Years Dioxide (TiO₂). *Toxicol. Appl. Pharmacol.* **79**, 179–192 (1985).
 14. LEE, K. P., TROCHIMOWICZ, H. J. & REINHARDT, C. F. PULMONARY RESPONSE OF RATS EXPOSED TO TITANIUM-DIOXIDE (TiO₂) BY INHALATION FOR 2 YEARS. *Toxicol. Appl. Pharmacol.* **79**, 179–192 (1985).
 15. Heinrich, U. *et al.* Chronic Inhalation Exposure of Wistar Rats and two Different Strains of Mice to Diesel Engine Exhaust, Carbon Black, and Titanium Dioxide. *Inhal. Toxicol.* **7**, 533 (1995).
 16. Kuempel, E. D., Tran, C. L., Castranova, V. & Bailer, a J. Lung dosimetry and risk assessment of nanoparticles: evaluating and extending current models in rats and humans. *Inhal. Toxicol.* **18**, 717–24 (2006).
 17. Walser, T. *et al.* Life-cycle assessment framework for indoor emissions of synthetic nanoparticles. *J. Nanoparticle Res.* **17**, 1–18 (2015).
 18. Nicas, M. Estimating Exposure Intensity in an Imperfectly Mixed Room. *Am. Ind. Hyg. Assoc. J.* **57**, 542–550 (1996).